Earth System Science Data

Paper # essd-2023-432

Jun. 11, 2024

Dear editor:

We would like to thank you for your constructive comments and suggested amendments on our manuscript. The comments are very useful for us to improve our research. We have carefully studied the comments and revised our manuscript accordingly.

Here are our detailed responses to your comments. Please note that the comments from you are in **bold font** followed by our responses in regular font, changes/additions to the manuscript are underlined.

Sincerely yours,

Wenping Yuan on behalf of all co-authors

Corresponding author: Wenping Yuan, Ph.D., Professor

School of Atmospheric Sciences,

Sun Yat-sen University

135 West Xingang Road, Guangzhou 510275, China

E-mail address: yuanwp3@mail.sysu.edu.cn

Detailed responses to editors' comments

We hope this message finds you well. Thank you for your efforts in revising the manuscript entitled "High-resolution mapping of global winter-triticeae crops using a sample-free identification method." We appreciate the substantial improvements made based on the previous round of feedback.

However, we believe there are still a few areas that would benefit from further clarification and enhancement. Specifically, the methodology section, particularly the calculation and application of the Winter-Triticeae Crops Index (WTCI), could be more detailed (section. 2.3 Method before Fig. 2a, 2b). Adding a visual representation, such as a flowchart, would significantly aid in understanding the steps involved in the WTCI calculation. In addition, while the validation process using various datasets is well-documented in the revised version, many if not all explanations were provided with little or no justification. Please provide more details on the selection criteria and the rationale behind using specific datasets. The selection criteria and the rationale would enhance the robustness and transparency of the study.

Considering these points, we suggest that the revised manuscript undergo another round of review to ensure that these critical aspects are fully addressed. This will help in confirming that the methodology is comprehensively understood and that the validation processes are thoroughly documented.

We appreciate your attention to these details and look forward to receiving the revised version of the manuscript.

Response: Thank you for your deep thought and suggestions. We have revised and added some details in method section, and a flowchart was drawn to represent the calculation and application process of the WTCI method. The details are as follows:

"**2.3 Method**

The workflow for identifying winter-triticeae crops (Fig. 2) mainly includes four steps after pre-processing satellite data: (1) selecting pixels with a maximum NDVI value greater than 0.4 during the winter-triticeae crops growing season as potential pixels; (2) developing the WTCI based on the unique characteristics of NDVI time series of winter-triticeae crops compared with other land cover types; (3) calculating the WTCI value of potential pixels to quantify their similarity with winter-triticeae crops, and using thresholds to obtain the distribution maps of winter-triticeae crops; (4) evaluating the performance of WTCI method based on validation data.

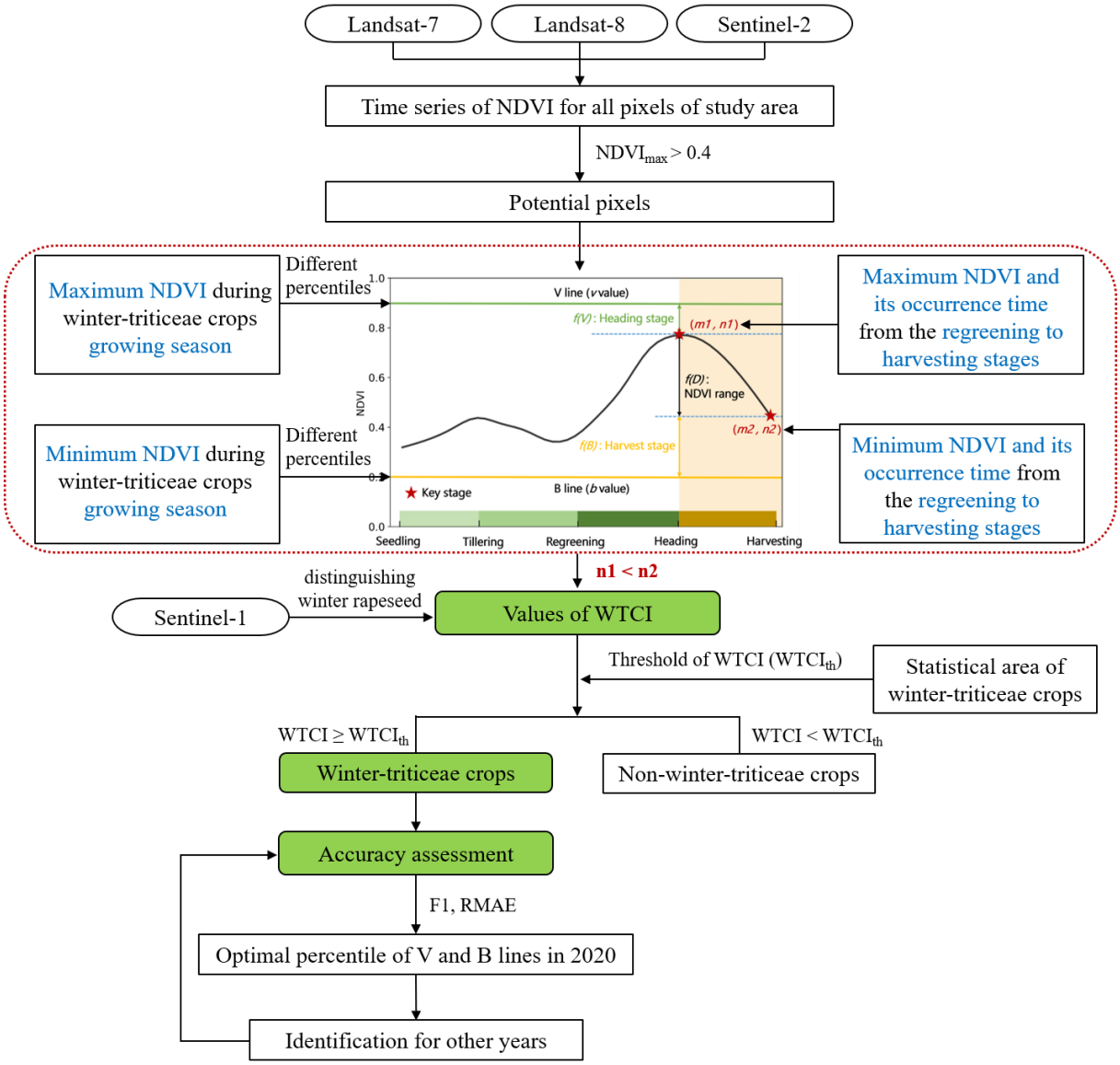

Figure 2: The flowchart of identifying winter-triticeae crops using the Winter-Triticeae Crops Index.

2.3.1 Time series characteristics of NDVI for different land cover types

The design of the Winter-Triticeae Crops Index (WTCI) is based on the analysis of NDVI

time series for different land cover types. Specifically, we first selected the NDVI time series of each pixel during the growth season (i.e., autumn to summer of the following year) of winter-triticeae crops. Pixels with NDVI greater than 0.4 are usually indicative of vegetation cover (Peng et al., 2019). Therefore, pixels with a maximum NDVI greater than 0.4 during the selected growth period were retained as the potential pixels. After applying these steps, the main remaining land cover types in the potential pixels were forest, grassland and cultivated land.

There are significant differences in the temporal variations of NDVI between winter-triticeae crops and natural vegetation types (i.e., deciduous forest, evergreen forest and grassland) during the growing season of winter-triticeae crops (Fig. 3b). Specifically, in the period from seedling to tillering stages, winter-triticeae crops are in a state of slow growth, with their NDVI gradually increasing. In contrast, natural vegetation types are in the deciduous stage, and exhibit a continuous decrease in NDVI during this period (Fig. 3b). From the regreening to the heading stages, the NDVI of winter-triticeae crops rapidly increases and reaches its maximum value, while the increase of NDVI of natural vegetation types tends to lag behind that of winter-triticeae crops (Fig. 3b). Furthermore, the NDVI of winter-triticeae crops show a downward trend and reach their lowest value during the harvesting stage. However, the NDVI values of natural vegetations rapidly increase at this time (Fig. 3b). Additionally, except for winter rapeseed, there are significant differences in the growth season of maize, rice and soybean compared to that of winter-triticeae crops. Therefore, these crops will not interfere with the identification of winter-triticeae crops, even if they have similarities in the NDVI time series characteristics with winter-triticeae crops.

Based on the above analysis, there are two periods that can be used to distinguish between winter-triticeae crops and natural vegetation types, i.e., the seedling to tillering stages and the heading to harvesting stages (Fig. 3b), during which the NDVI of winter-triticeae crops and natural vegetation types showed opposite temporal variations. Compared with the period from seedling to tillering, the NDVI characteristics of winter-triticeae crops from heading to harvesting stages are more stable, and more significantly different from those of natural vegetation types. A previous study on the relatively weak growth and not obvious increase of

NDVI of winter-triticeae crops from seedling to tillering stages (Wang et al., 2015) further supports our finding. Therefore, this study used the NDVI time series characteristics of winter-triticeae crops from heading to harvesting stages to design the WTCI.

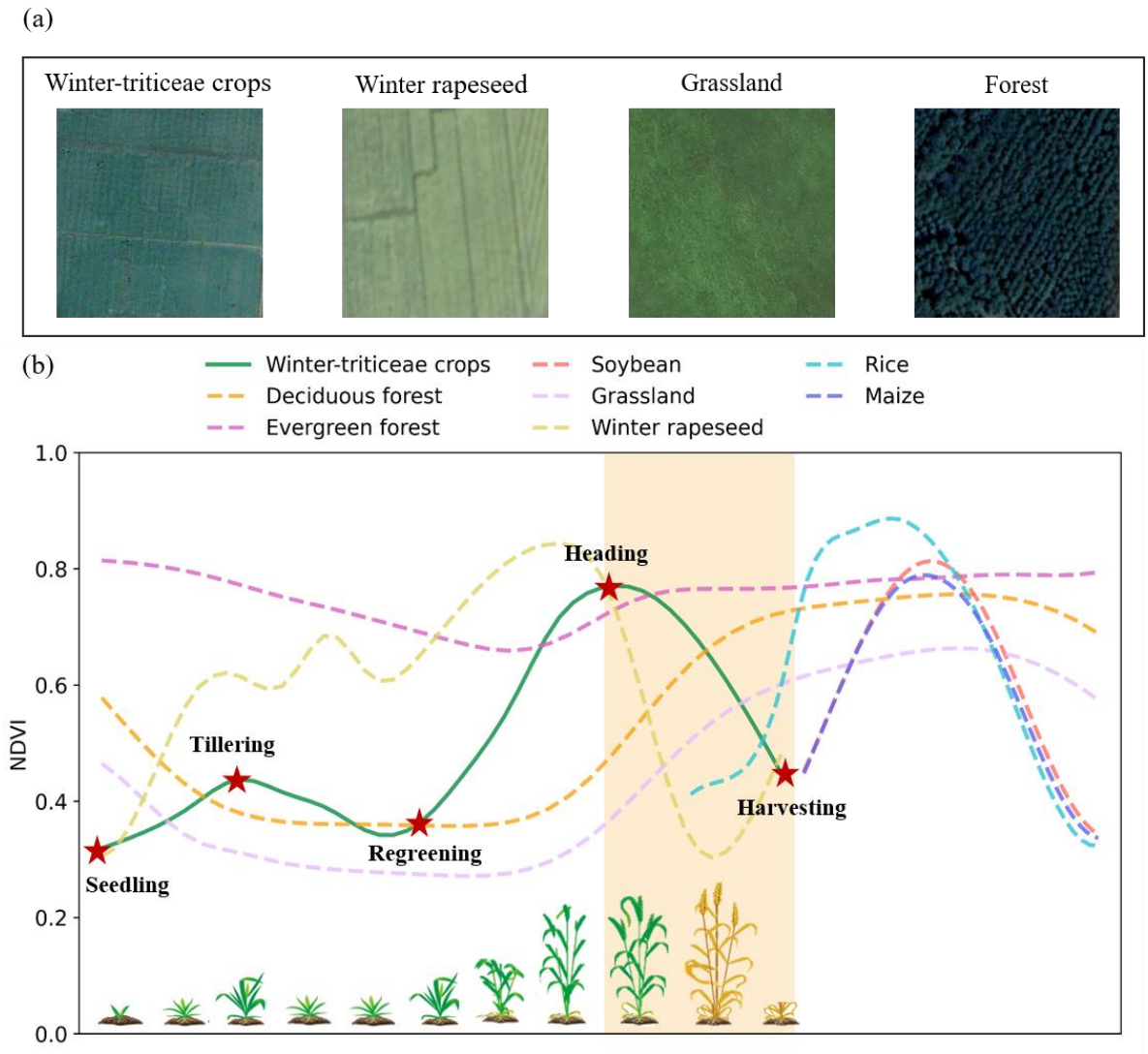

Figure 3: Example of the (a) textures and colours on the high-resolution images from © Google Earth and (b) NDVI time series characteristics of different land cover types. The red five-pointed stars represent the different phenological stages of winter-triticeae crops.

2.3.2 Development of the Winter-Triticeae Crops Index

Based on the comparison of the NDVI time series characteristics of winter-triticeae crops with natural vegetation types, the unique characteristics of winter-triticeae crops during the growing season can be summarized as: (1) the NDVI of winter-triticeae crops peaks at the heading stage, which is close to the maximum value of natural vegetation during its growing

season; (2) winter-triticeae crops have low NDVI values during the harvesting stage, when the surface tends to be close to bare land after crop removal. On the contrary, the NDVI of natural vegetation approaches its peak in a year. To quantify the above characteristics, this study set an upper boundary to denote vegetation (V line) and a lower boundary to indicate bare land (B line) (Fig. 4). Then, three indicators, $f(D)$, $f(V)$, and $f(B)$, were constructed to represent the unique NDVI characteristics of winter-triticeae crops from the heading to the harvesting stages (Fig. 4), and their integrate (i.e., WTCI) were employed to determine whether the potential pixel is winter-triticeae crops:

$$WTCI = f(D) \times f(V) \times f(B), n1 < n2 \ , \quad (1)$$

where *n1* and *n2* represent the time when the maximum and minimum NDVI appear, respectively (Fig. 4). It should be noticed that Eq. (1) was used to identify the winter-triticeae crops only when *n1*<*n2*, i.e., the maximum NDVI should appear before the minimum NDVI. Specifically, $f(D)$, $f(V)$, and $f(B)$ were designed as follows:

$$f(D) = \frac{1}{1+e^{\left(\frac{v-b}{2}-D\right)}}, D = m1 - m2 \ , \quad (2)$$

$$f(V) = 1 - V^2, V = \begin{cases} 1, \ m1 \le b \\ \frac{v-m1}{v-b}, b < m1 \le v \\ 0, \ m1 > v \end{cases} , \quad (3)$$

$$f(B) = 1 - B^2, B = \begin{cases} 1, m2 \ge v \\ \frac{m2-b}{v-b}, b \le m2 < v \\ 0, m2 < b \end{cases} , \quad (4)$$

where *v* and *b* represent the NDVI corresponding to the V and B lines, respectively. *m1* and *m2* represent the maximum and minimum NDVI of the potential pixel from the heading to harvesting stages (Fig. 4), respectively. f (D) quantifies the proximity of the range of NDVI variation between the potential pixels and those of winter-triticeae crops. Given a pixel with *D* (i.e., *m1 – m2*) closer to the value of *v – b*, the higher the value of $f(D)$, the higher the likelihood that it represents a winter-triticeae crops. $f(V)$ quantifies the proximity of the maximum NDVI (*m1*) of the potential pixels with that of vegetation. The pixels closer to the V line at the *n1* period (i.e., *m1* approaches *v*) are more likely to be winter-triticeae crops. Additionally, $f(B)$ quantifies the proximity of the minimum NDVI (*m2*) of the potential pixel with that of bare land. Pixels closer to the B line at the *n2* period (i.e., *m2* approaches *b*) have a greater likelihood

of being winter-triticeae crops. The algorithms of $f(D)$, $f(V)$, and $f(B)$ reported by Xu et al. (2023) were used in this study.

Winter-triticeae crops should simultaneously have all the above three characteristics, this means that the WTCI should be designed to integrate these three indicators. The values of $f(D)$, $f(V)$ and $f(B)$ range from 0 to 1. Therefore, WTCI varies between 0 and 1, and pixels with higher WTCI have a greater probability of being winter-triticeae crops. In addition, this study uses agricultural statistical data to determine the threshold of WTCI. When the WTCI of the potential pixel is greater than or equal to this threshold, it is considered a winter-triticeae crop pixel.

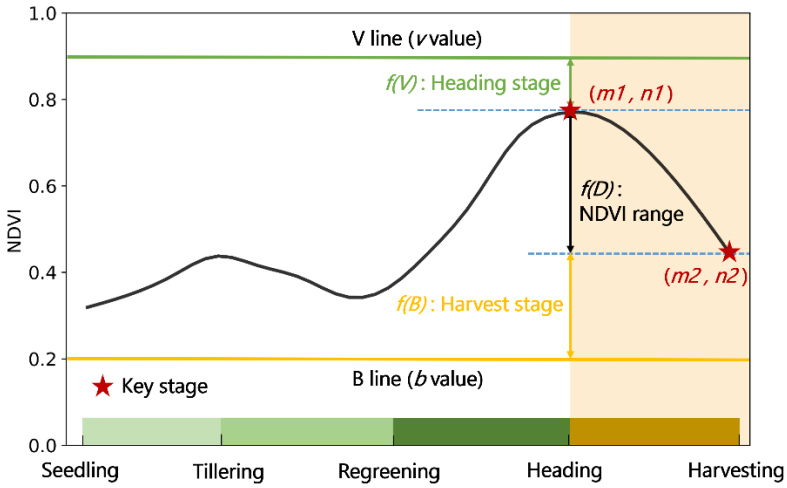

Figure 4: Characteristics of NDVI time series for designing the Winter-Triticeae Crops Index. The black solid line represents the NDVI time series of winter-triticeae crops. The green and orange solid lines represent the V line and the B line, respectively; The red five-pointed stars indicate the heading and harvesting stages of winter-triticeae crops; *m1* and *n1* represent the maximum value of NDVI and the time when the maximum value occurs during the study period; *m2* and *n2* represent the minimum value of NDVI and the time when the minimum value occurs during the study period.

2.3.3 WTCI-based winter-triticeae crops identification

In this study, we considered each state (or province) as an identification unit in China, Brazil, India, Australia and US, and the threshold of WTCI was determined based on statistical area at state (or province) scale. For the remaining countries, we treated each country as an identification unit, and the threshold of WTCI was calculated relied on statistical area at national scale. Furthermore, given the diversity and complexity of land cover types and

agricultural planting structures in the study area, we used different percentile combinations of the V and B lines. Specifically, this study referred to crop calendar data provided by the United States Department Agriculture (USDA) (https://ipad.fas.usda.gov/ogamaps/cropcalendar.aspx) to determine the growth season of winter-triticeae crops in each country. Then, we extracted the maximum and minimum NDVI of all potential pixels in each identification unit during the growing season of winter-triticeae crops. We further obtained different percentiles (5%, 20%, 40%, 60%, 80% and 95%) of the maximum and minimum NDVI for each identification unit, respectively, corresponding to *v* and *b* in the Eq. (2), Eq. (3) and Eq. (4). In addition, the *m1* and *m2* were automatically searched in the NDVI curve between the regreening and harvesting stages of winter-triticeae crops. In this study, the regreening stage was based on the start time of spring in the northern (March) and southern (September) hemispheres (Ren et al., 2019), and the harvesting stage referred to the crop calendar provided by USDA. We first determined the *m1* and *n1* of each potential pixel, then we looked for the *m2* in the period after *n1*, and further calculated WTCI. Pixels that do not meet this condition (i.e., $n1<n2$) are identified as non-winter-triticeae crops. In addition, we determined the optimal combination of V and B lines in each identification unit according to the identification accuracy at the pixel scale (F1 score) and the relative mean absolute error (RMAE) between identified and agricultural statistical areas. For countries lacking agricultural statistical data, the optimal combination was decided solely based on the F1 score. Based on the optimal combination of V and B lines of each identification unit in 2020, winter-triticeae crops from 2017 to 2019 and 2021 to 2022 were identified to evaluate the temporal transferability of the WTCI.

The identification of winter-triticeae crops in the study area may be affected by winter rapeseed and garlic, as these crops have similar growth season and spectral characteristics with winter-triticeae crops (Fu et al., 2023b; Tian et al., 2021). Winter rapeseed is mainly distributed in China, India and parts of Europe. The planting area of winter rapeseed in some states (or provinces) of China and India is equivalent to or even higher than that of winter-triticeae crops, while the planting area in countries, such as France, Germany, Poland, Britain, Hungary and Ukraine, accounts for 17%-32% of the planting area of winter-triticeae crops. Winter garlic is mainly distributed in some provinces of China, Spain and Ukraine. However, the planting area

of winter garlic is very small compared to that of winter-triticeae crops and winter rapeseed. For example, the planting area of winter garlic in China, the largest planting country, only accounted for about 2% of the winter crops (http://data.stats.gov.cn/). Therefore, this study only distinguished between winter rapeseed and winter-triticeae crops. The NDVI time series of winter rapeseed shows a downward trend from the heading to harvest stages of winter-triticeae crops, which is resemble winter-triticeae crops (Fig. 3b). Tao et al. (2023) have also demonstrated that winter rapeseed and winter-triticeae crops have similar NDVI characteristics, making it difficult to distinguish them only based on optical images (Veloso et al., 2017). Fortunately, previous studies have indicated that the VH (vertical transmit and horizontal receive) band can effectively eliminate the interference from winter rapeseed in the identification of winter-triticeae crops in China and Europe (Dong et al., 2020a; Huang et al., 2022). Therefore, we distinguished winter rapeseed and winter-triticeae crops based on the methods of these studies. Specifically, the VH threshold set by Dong et al. (2020a), which was obtained by comparing winter-triticeae crops and winter rapeseed filed samples, was employed in this study. In regions of India where winter rapeseed is planted, we calculated the VH values from Sentinel-1 images in March considering the lower latitude and earlier harvest period of these regions. In other Asian regions where winter rapeseed is grown, this study obtained VH values for April. This study identified these pixels with VH values greater than -15.5 in March or April as non-winter-triticeae crops. Similarly, in some European countries, we calculated VH values for May, and considered that pixels with VH values greater than -15.5 were non-winter-triticeae crops (Huang et al., 2022)."

In addition, we have added more details on the selection criteria and the rationale behind using various validation samples, and the details are as follows:

"The validation samples were obtained from: (1) field surveys, (2) Google Earth images, (3) CDL dataset and (4) LPIS dataset. We conducted field surveys in Hebei, Henan, Shandong, Anhui, and Jiangsu provinces in China in 2019 and 2020. The survey routes were pre-planned based on prior knowledge of the spatial distribution of winter-triticeae crops and transportation accessibility. In the fieldwork, we only selected large winter-triticeae crops fields with an area great than 900 m^2, and used GPS (G120, UniStrong, Beijing, China) (Fu et al., 2023b) to mark

the locations inside the fields. For non-winter-triticeae crops samples, we randomly selected large areas of non-winter-triticeae crops fields, forests, and grasslands around the pre-planned routes, and also used GPS to mark their locations. Finally, we processed these samples using Acrmap10.2 to maintain the same spatial projection as the identification map in China, resulting in a total of 3,054 winter-triticeae crops samples and 4,088 non-winter-triticeae crops samples. For other provinces in China and other countries (except US), we relied on high-resolution images from Google Earth from 2019 to 2020 for visual interpretation, which is a compensatory and effective method when ground truth samples cannot be obtained (Huang et al., 2022; Zheng et al., 2022). We first chose regions with available images during the growing season of winter-triticeae crops (section 2.3.3), and selected samples from these regions based on the texture features and colours. Winter-triticeae crops have deeper colour or stronger texture than winter rapeseed and grassland, and their roughness is lower than that of forest, which can be used to distinguish winter-triticeae crops from other land cover types (Fig .3a). Crops with different growing season (such as maize, rice and soybean) will not affect the visual interpretation. To ensure the accuracy of the samples, we then validated the selected samples on GEE platform by checking whether the NDVI temporal features of these samples matched the characteristics of winter-triticeae crops, and finally obtained 7,029 winter-triticeae crops samples and 8,897 non-winter-triticeae crops samples (Fig. 1).

In addition, we used CDL and LPIS datasets to further evaluate the performance of WTCI method. The CDL released annually has high accuracy in capturing crop distribution in US and has been widely used as a base map for crop dynamic monitoring and production estimation (Wang et al, 2019; Xu et al., 2023). We thus treated CDL labels as ground truth to validate the accuracy of our identification map in the US. Specifically, we first used Acrmap10.2 to randomly select samples from pixels labelled with winter-triticeae crops, including winter wheat, double crop winter wheat/soybeans, winter wheat/corn, winter wheat/sorghum and winter wheat/cotton. Non-winter-triticeae crops samples were randomly generated in the remaining pixels. Then we converted these samples into the same spatial projection as the identification map in the US. We finally obtained 7,500 winter-triticeae crops samples and 12,500 non-winter-triticeae crops samples in 2020 (Fig. 1). The LPIS dataset, produced by

European Union, accurately records and describes field location and land cover in EU countries, and represents the optimum available data on the spatial distribution of crops in these countries (Ballot et al., 2023). We collected 10 countries (Austria, Belgium, Germany, Denmark, Estonia, France, Netherlands, Slovakia, Slovenia and Sweden) with winter-triticeae crops clearly labelled in LPIS dataset, including winter spelt, winter barley, winter durum hard wheat, winter common soft wheat, winter triticale, winter rye and winter oats (https://zenodo.org/records/10118572), and these data cover the period from 2018 to 2021. We first randomly extracted winter-triticeae crops samples and non-winter-triticeae crops samples from each country using Acrmap 10.2. We then transformed the spatial projection of these samples to be consistent with the European identification map, and ultimately obtained 2,000 winter-triticeae crops samples and 3,000 non-winter-triticeae crops samples to assess the result of WTCI method in Europe (Fig. 1).”

References:

Ballot, R., Guilpart, N., Jeuffroy, M.-H.: The first map of crop sequence types in Europe over 2012–2018, Earth Syst. Sci. Data, 15, 5651–5666, https://doi.org/10.5194/essd-15-5651-2023, 2023.

Wang, S., Azzari, G., Lobell, D. B.: Crop type mapping without field-level labels: Random forest transfer and unsupervised clustering techniques, Remote Sens. Environ., 222, 303-317, https://doi.org/10.1016/j.rse.2018.12.026, 2019.